Experimental test rig designed to analyse pumping station operation controlled by pressure at different key points

Petre-Ovidiu Ciuc[1], *Remus Alexandru* Mădulărea[1], *Andrei-Mugur* Georgescu[2], *Mihaela Amalia* Diminescu[1], and *Sanda-Carmen* Georgescu[1,*]

[1]University POLITEHNICA of Bucharest, Power Engineering Faculty, 313 Spl. Independentei, 060042, Bucharest, Romania
[2]Technical University of Civil Engineering Bucharest, Hydraulics and Environmental Protection Department, 124 Lacul Tei, 020396, Bucharest, Romania

Abstract. The operation of pumps within a pumping station can be controlled by the Pressure Set Point (PSP) value compared to the reading of a pressure sensor placed either at the exit of the pumping station, on the main discharge pipe (*classical PSP method*), or at a critical/monitoring point within the water distribution network (termed further as *remote-control PSP method*). We designed and built an experimental test rig, allowing to study both control methods, in the attempt to check the advantage of the *remote-control PSP method*, with respect to the *classical PSP method*, since governing equations show that they are equivalent. The design relies on the theoretical approach and numerical results presented within this paper.

1 Introduction

Excessive operating pressure in Water Distribution Networks (WDN) induces stress on pipes and thus increases the risk of leakages and bursts [1, 2], while the energy consumed for pumping is wasted unnecessarily. The overall effect is a rise of the WDNs' operation, maintenance and repairing costs [3]. Conversely, insufficient pressure in WDN induces water demand shortage at the consumers. Therefore, water companies need to optimise the pressure in the supplied network, depending on the requested variable demand.

Generally, in a Pumping Station (PS), pumps operation is controlled by the pressure value measured by a pressure sensor on the PS main discharge pipe. The system pressure must be kept around a so-called Pressure Set Point (PSP) – a pressure level at which the pressure switch is adjusted to actuate on rising or falling pressure (a small adjustable pressure range includes that level). One can keep the PSP level by successively switching on or off certain pumps. Variable speed driven pumps allow smooth adjustments of pump speed in order to reach the PSP level [4, 5]. Within the WDN design phase, the PSP value can be computed using hydraulic analysis; for an existing WDN, with predictable water consumption, the PSP value selection can rely on historical or archived data. The above control method, based on the PSP value compared to the reading of a pressure sensor placed at the exit of the pumping station, on the main discharge pipe, will be termed further as *classical PSP method*. Although simple and easy to implement, it was proved that the *classical PSP method* usually ensures an excessive pressure across the WDN, greater than the level requested by the end-users (consumers).

To avoid exceeding pressure at the end-users, one can choose to control the pumps operation within a PS with respect to a PSP value compared to the reading of a pressure sensor positioned at a critical point (monitoring node) within the WDN. For WDNs fed by multiple pumping stations, each PS can be controlled by its own PSP level, compared to pressure values measured at a critical point that is 100% fed by the considered PS [6, 7]. The latter control method implies remote-control (i.e. real time data acquisition and transmission); thus, it will be termed further as *remote-control PSP method*. Due to additional costs attached to the remote-control, that method might be less appealing for water companies.

In order to verify if there is any advantage of the *remote-control PSP method*, with respect to the *classical PSP method*, we designed and built an experimental test rig, that can be adapted to study both control methods. This paper focuses on the theoretical approach and numerical results that allowed us to design the test rig.

2 Experimental test rig description

An experimental setup was designed and recently built, to test a pumping station in a pipe network, when the PS operation is controlled either by the *classical PSP method*, or by the *remote-control PSP method*. The above experimental facility is located at the University "Politehnica" of Bucharest [8]. The studied pumping station [9] is equipped with 3 parallel-coupled pumps (of vertical centrifugal type), each with variable frequency drive. Technical details related to that PS can be found in Dunca et al. [10]. The scheme of the test rig is presented in figure 1, where pumps are denoted as P1, P2 and P3.

---

*
Corresponding author: carmen.georgescu@upb.ro
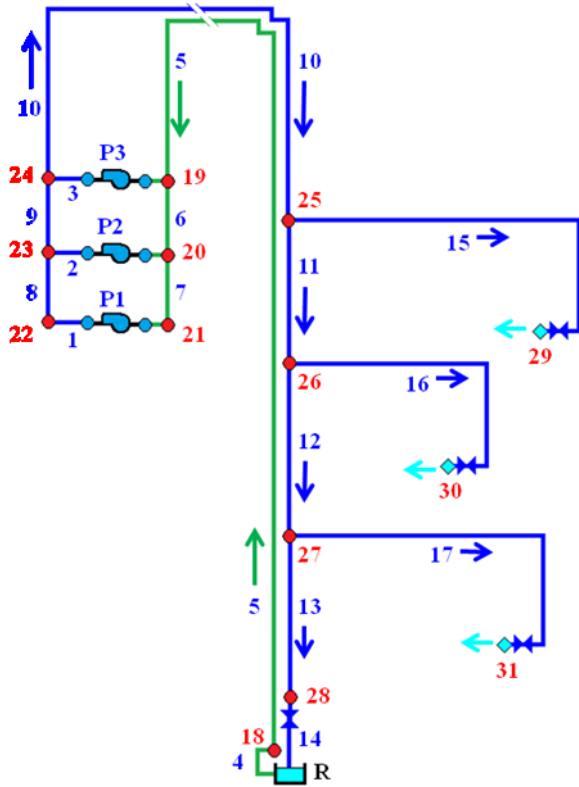
Fig. 1. Scheme of the experimental test rig: open tank R; pumps P1 to P3; 17 pipes ($j = 1 \div 17$) and 14 nodes ($j = 18 \div 31$); the last 3 nodes ($j = 29 \div 31$) are the consumers.

The pumping station is fed through a main suction pipe from the open tank R (with a capacity of 75 litres, open to the atmosphere). There are 3 consumers (placed at nodes $29 \div 31$), each fed through a pipe that branches out from the main discharge pipe. A Throttle Control Valve (TCV) allows establishing a certain outflow rate at each consumer. In order to keep a constant water level in the tank, the flowing jets are redirected to the tank using a gutter channel (figure 2). The remaining flow rate (the difference between the pumped flow rate and the outflows at the consumers) enters the tank through the pipe 14. The downstream TCV placed on pipe 14 is used to control the flow rate in the hydraulic system.

Fig. 2. Flowing water jets collected into the gutter channel.

Tables 1 and 2 contain the network geometrical data: length L_j and inner diameter D_j of pipes with $j = 1 \div 17$, and elevation z_j of 14 nodes with $j = 18 \div 31$. To simplify notations, for $j = 1 \div 3$, we considered that the pipe j has 2 components: one attached to the suction side (s) and the other attached to the discharge side (d) of the pump (thus, the pipes with $j = 1 \div 3$ are bordered each by the pair of nodes 19 & 24; 20 & 23; 21 & 22, as in figure 1).

Table 1. Pipe length L_j (in meters) and inner diameter D_j (in millimetres), where $j = 1 \div 17$. For $j = 1 \div 3$, there are two components: s on the suction side and d on the discharge side of the designated pump (P1÷P3).

pipe ID j	L_j [m]	D_j [mm]	pipe ID j	L_j [m]	D_j [mm]
1s (P1)	0.15	36.6	8	0.32	42.5
1d (P1)	0.37	27.9	9	0.32	42.5
2s (P2)	0.15	36.6	10	10.845	29.2
2d (P2)	0.37	27.9	11	0.44	29.2
3s (P3)	0.15	36.6	12	0.92	29.2
3d (P3)	0.37	27.9	13	1.225	29.2
4	0.825	36.5	14	0.28	36.5
5	13.44	29.2	15	2.04	18.2
6	0.32	42.5	16	1.755	18.2
7	0.32	42.5	17	1.97	18.2

Table 2. Node elevation z_j (in meters above the floor level).

Node (nodes) ID j	z_j [m]	Node (nodes) ID j	z_j [m]
18-21	0.23	upstream TCV 30	1.27
22-28	0.53	30 (TCV's exit)	1.055
upstream TCV 29	1.57	upstream TCV 31	1.5
29 (TCV's exit)	1.355	31 (TCV's exit)	1.285

An equivalent roughness of 0.1 mm is considered on all pipes. The head of the open tank is $H_R = 0.77$ m; it is kept constant.

The speed factor ω is the ratio between the actual speed and the nominal speed of the pump. The head – flow rate curve, and the efficiency curve of the pumps P1÷P3 running at a certain speed are defined as in [10]:

$$H_{Pj} = H_{Pj}(Q_j) = 31.62\,\omega_j^2 - 17.625 \cdot 10^6 Q_j^2 \qquad (1)$$

$$\eta_j = \eta_j(Q_j) = 1647 Q_j / \omega_j - 1.28 \cdot 10^6 (Q_j / \omega_j)^2 \quad (2)$$

for $j = 1 \div 3$, with the pumping head H in meters, flow rate Q in m³/s and dimensionless efficiency η. The cavitation curve of the pumps P1÷P3 running at their nominal speed is fitted by a polynomial regression curve:

$$NPSH_j = 5.04 - 1.27 \cdot 10^4 Q_j + 8 \cdot 10^6 Q_j^2 + 7.5 \cdot 10^9 Q_j^3 \quad (3)$$

with the net positive suction head *NPSH* in meters, for the flow rate Q in m³/s.

3 Theoretical approach

To design the test rig from figure 1, we will assume that all 3 pumps run at their nominal speed, and all valves are

fully open, namely the TCV (of DN50 size) on pipe 14 and the TCVs (of DN25 size) at nodes 29÷31.

At each consumer ($j = 29÷31$), the requested demand is $Q_r = 0.27 \cdot 10^{-3}$ m^3/s = 0.972 m^3/h (it corresponds to an economic velocity [4] at the valve of DN25 size). The available water demand Q_a is computed with a pressure-demand relationship [11-13], as:

$$Q_a = Q_r \times \begin{cases} 1 & \text{if } p \geq p_{ref} \\ \sqrt{\dfrac{p - p_{min}}{p_{ref} - p_{min}}} & \text{if } p_{min} \leq p < p_{ref} \\ 0 & \text{if } p < p_{min} \end{cases} \qquad (4)$$

where p (in meters of water column) is the available pressure at the consumer, p_{ref} is the reference gauge pressure (requested to ensure the outflow Q_r) and p_{min} is the minimal gauge pressure for which an outflow exists. For the studied test rig, $p_{ref} = 2$ mWC and $p_{min} = 0$ mWC. The available pressure head is $p_j/(\rho g) = (H_j - z_j)$, for $j = 29÷31$, where H is the nodal head (in meters), ρ is the water density and g is the gravity.

Head losses on pipes are computed with the Darcy-Weisbach formula, as $R_j Q_j^2$ for $j = 1÷17$, where R is the hydraulic resistance (in s^2/m^5) and Q is the flow rate (in m^3/s). The fiction factor is computed using the Swamee and Jain formula [14]. Minor losses will be considered only at the TCV on pipe 14, as $R_v Q_{14}^2$, where the local hydraulic resistance R_v depends on the minor loss coefficient ζ. When that valve is fully open (as for the present design assumptions), then $\zeta = 0$; in section 4, that valve will be partially closed ($\zeta > 0$). To simplify the hydraulic analysis, any other minor losses, as well as the inlet and outlet kinetic terms on pipes, will be further neglected (for the studied test rig, these assumptions, valid for $L_j/D_j > 200$ [4], fit only the main suction pipe with $j = 5$ and the main discharge pipe with $j = 10$).

For the test rig (fig. 1), 17 energy balance equations resulted for the flow through pumps P1÷P3 (with flow rates $Q_1÷Q_3$ and pumping heads $H_{P1}÷H_{P3}$ defined by (1)) and for the flow through the remaining 14 pipes with $j = 4÷17$. The system contains 14 additional continuity equations in nodes with $j = 18÷31$, where for the last 3 nodes (consumers), relation (4) applies. Considering that all pumps run at nominal speed, their speed factors are set to $\omega_j = 1$ in (1), for $j = 1÷3$. The following system of 31 equations, with 31 unknowns (17 flow rates Q_j for $j = 1÷17$, and 14 nodal heads H_j for $j = 18÷31$) resulted:

$$f_1 = H_{21} + 31.62\omega_1^2 - 17.625 \cdot 10^6 Q_1^2 - H_{22} - R_1 Q_1^2 = 0$$
$$f_2 = H_{20} + 31.62\omega_2^2 - 17.625 \cdot 10^6 Q_2^2 - H_{23} - R_2 Q_2^2 = 0$$
$$f_3 = H_{19} + 31.62\omega_3^2 - 17.625 \cdot 10^6 Q_3^2 - H_{24} - R_3 Q_3^2 = 0$$
$$f_4 = H_R - H_{18} - R_4 Q_4^2 = 0$$
$$f_5 = H_{18} - H_{19} - R_5 Q_5^2 = 0 \qquad (5)$$
$$f_6 = H_{19} - H_{20} - R_6 Q_6^2 = 0$$
$$f_7 = H_{20} - H_{21} - R_7 Q_7^2 = 0$$

$$f_8 = H_{22} - H_{23} - R_8 Q_8^2 = 0$$
$$f_9 = H_{23} - H_{24} - R_9 Q_9^2 = 0$$
$$f_{10} = H_{24} - H_{25} - R_{10} Q_{10}^2 = 0$$
$$f_{11} = H_{25} - H_{26} - R_{11} Q_{11}^2 = 0$$
$$f_{12} = H_{26} - H_{27} - R_{12} Q_{12}^2 = 0$$
$$f_{13} = H_{27} - H_{28} - R_{13} Q_{13}^2 = 0$$
$$f_{14} = H_{28} - H_R - (R_{14} + R_v) Q_{14}^2 = 0$$
$$f_{15} = H_{25} - H_{29} - R_{15} Q_{15}^2 = 0$$
$$f_{16} = H_{26} - H_{30} - R_{16} Q_{16}^2 = 0$$
$$f_{17} = H_{27} - H_{31} - R_{17} Q_{17}^2 = 0$$
$$f_{18} = Q_4 - Q_5 = 0$$
$$f_{19} = Q_5 - Q_3 - Q_6 = 0$$
$$f_{20} = Q_6 - Q_2 - Q_7 = 0$$
$$f_{21} = Q_7 - Q_1 = 0$$
$$f_{22} = Q_1 - Q_8 = 0$$
$$f_{23} = Q_8 + Q_2 - Q_9 = 0$$
$$f_{24} = Q_9 + Q_3 - Q_{10} = 0$$
$$f_{25} = Q_{10} - Q_{11} - Q_{15} = 0$$
$$f_{26} = Q_{11} - Q_{12} - Q_{16} = 0$$
$$f_{27} = Q_{12} - Q_{13} - Q_{17} = 0$$
$$f_{28} = Q_{13} - Q_{14} = 0$$

if $(H_{29} - z_{29}) \geq p_{ref}/(\rho g)$, $f_{29} = Q_{15} - Q_r = 0$

if $p_{min}/(\rho g) \leq (H_{29} - z_{29}) < p_{ref}/(\rho g)$,

$$f_{29} = Q_{15} - Q_r \sqrt{\dfrac{(H_{29} - z_{29}) - \dfrac{p_{min}}{\rho g}}{\dfrac{p_{ref}}{\rho g} - \dfrac{p_{min}}{\rho g}}} = 0 \qquad (5)$$

if $(H_{29} - z_{29}) < p_{min}/(\rho g)$, $f_{29} = Q_{15} = 0$

if $(H_{30} - z_{30}) \geq p_{ref}/(\rho g)$, $f_{30} = Q_{16} - Q_r = 0$

if $p_{min}/(\rho g) \leq (H_{30} - z_{30}) < p_{ref}/(\rho g)$,

$$f_{30} = Q_{16} - Q_r \sqrt{\dfrac{(H_{30} - z_{30}) - \dfrac{p_{min}}{\rho g}}{\dfrac{p_{ref}}{\rho g} - \dfrac{p_{min}}{\rho g}}} = 0$$

if $(H_{30} - z_{30}) < p_{min}/(\rho g)$, $f_{30} = Q_{16} = 0$

if $(H_{31} - z_{31}) \geq p_{ref}/(\rho g)$, $f_{31} = Q_{17} - Q_r = 0$

if $p_{min}/(\rho g) \leq (H_{31} - z_{31}) < p_{ref}/(\rho g)$,

$$f_{31} = Q_{17} - Q_r \sqrt{\dfrac{(H_{31} - z_{31}) - \dfrac{p_{min}}{\rho g}}{\dfrac{p_{ref}}{\rho g} - \dfrac{p_{min}}{\rho g}}} = 0$$

if $(H_{31} - z_{31}) < p_{min}/(\rho g)$, $f_{31} = Q_{17} = 0$.

The nonlinear system of equations (5) contains two type of unknowns: flow rates and nodal heads. To solve it, all unknowns will be denoted as w_j with $j = 1÷31$:

$$w_1, w_2, \cdots, w_{17} \equiv Q_1, Q_2, \cdots, Q_{17}$$
$$w_{18}, w_{19}, \cdots, w_{31} \equiv H_{18}, H_{19}, \cdots, H_{31} \tag{6}$$

Thus, the system of equations (5) becomes:

$$f_1 = w_{21} + 31.62\omega_1^2 - 17.625 \cdot 10^6 w_1^2 - w_{22} - R_1 w_1^2 = 0$$
$$f_2 = w_{20} + 31.62\omega_2^2 - 17.625 \cdot 10^6 w_2^2 - w_{23} - R_2 w_2^2 = 0$$
$$f_3 = w_{19} + 31.62\omega_3^2 - 17.625 \cdot 10^6 w_3^2 - w_{24} - R_3 w_3^2 = 0$$
$$\cdots\cdots$$
$$f_9 = w_{23} - w_{24} - R_9 w_9^2 = 0$$
$$f_{10} = w_{24} - w_{25} - R_{10} w_{10}^2 = 0$$
$$\cdots\cdots$$
$$f_{13} = w_{27} - w_{28} - R_{13} w_{13}^2 = 0 \tag{7}$$
$$f_{14} = w_{28} - H_R - (R_{14} + R_v) w_{14}^2 = 0$$
$$\cdots\cdots$$

if $(w_{31} - z_{31}) \geq p_{ref}/(\rho g)$, $f_{31} = w_{17} - Q_r = 0$

if $p_{min}/(\rho g) \leq (w_{31} - z_{31}) < p_{ref}/(\rho g)$,

$$f_{31} = w_{17} - Q_r \sqrt{\frac{(w_{31} - z_{31}) - \dfrac{p_{min}}{\rho g}}{\dfrac{p_{ref}}{\rho g} - \dfrac{p_{min}}{\rho g}}} = 0$$

if $(w_{31} - z_{31}) < p_{min}/(\rho g)$, $f_{31} = w_{17} = 0$.

The system (7) can be compacted as **f(w) = 0**, where the column vector **w** contains 31 components w_j and the column vector **f** contains 31 components, namely the functions $f_j(w_1, w_2, ..., w_{31}) = 0$, with $j = 1 \div 31$.

Further, the nonlinear system (7) was solved in GNU Octave [4, 15], using the built-in function *fsolve* (also available in MATLAB [16]); *fsolve* requests a user-supplied initial solution (starting guess), denoted here by a column vector **w0** of 31 components w_{0j}. It turned out that the above nonlinear system was not at all sensitive to the initial solution. The final solution **w** of the system (7), obtained for **w0** with all components equal to zero ($w_{0j} = 0$, for $j = 1 \div 31$), is presented in table 3.

In table 3, flow rates $w_j = Q_j$ for $j = 1 \div 17$ are presented both in m³/s and m³/h. The last 3 flow rate values equal the corresponding available demand in nodes 29 to 31: $Q_{15} = Q_{a29}$; $Q_{16} = Q_{a30}$ and $Q_{17} = Q_{a31}$. All 3 outflow rates are smaller than the imposed requested demand Q_r – this is consistent with the available pressure heads at the consumers, which are below the reference pressure head of 2 m.

Based on the parameters attached to the duty point of each pump (table 4): computed flow rate Q_j, pumping head H_{Pj} (1) and pump efficiency η_j (2) for $\omega_j = 1$, the power P_j of each pump, for $j = 1 \div 3$ can be computed, as:

$$P_j = \rho g Q_j H_j / \eta_j . \tag{8}$$

The total power consumed for pumping is $P_T = 1117$ W. The duty points of the pumps are located towards the end of the head – flow rate curve (1), where the efficiency drops to 37%. Obviously, the operation of pumps at full capacity within the designed network is not

the best choice, so in the future, it will be suitable to conduct most of the experimental tests with the discharge valve on pipe 14 partially closed ($\zeta \neq 0$).

Table 3. Numerical solution of the system (7), for $\zeta = 0$: w_j for $j = 1 \div 31$ and available pressure head $p_j/(\rho g)$ for $j = 29 \div 31$.

$w_j = Q_j$ for $j = 1 \div 17$		Q_j [m³/h]	$w_j = H_j$ for $j = 18 \div 31$ [m]	
w_1	Q_1	0.00099	3.580	w_{18}	H_{18}	0.516
w_2	Q_2	0.00099	3.581	w_{19}	H_{19}	-0.737
w_3	Q_3	0.00100	3.585	w_{20}	H_{20}	-0.757
w_4	Q_4	0.00298	10.745	w_{21}	H_{21}	-0.763
w_5	Q_5	0.00298	10.745	w_{22}	H_{22}	13.372
w_6	Q_6	0.00199	7.160	w_{23}	H_{23}	13.367
w_7	Q_7	0.00099	3.580	w_{24}	H_{24}	13.346
w_8	Q_8	0.00099	3.580	w_{25}	H_{25}	2.700
w_9	Q_9	0.00199	7.160	w_{26}	H_{26}	2.325
w_{10}	Q_{10}	0.00298	10.745	w_{27}	H_{27}	1.652
w_{11}	Q_{11}	0.00277	9.990	w_{28}	H_{28}	0.829
w_{12}	Q_{12}	0.00257	9.250	w_{29}	H_{29}	2.563
w_{13}	Q_{13}	0.00246	8.857	w_{30}	H_{30}	2.212
w_{14}	Q_{14}	0.00246	8.857	w_{31}	H_{31}	1.613
w_{15}	Q_{15}	0.00021	0.755	$p_{29}/(\rho g)$ [m]		1.208
w_{16}	Q_{16}	0.00021	0.739	$p_{30}/(\rho g)$ [m]		1.157
w_{17}	Q_{17}	0.00011	0.393	$p_{31}/(\rho g)$ [m]		0.328

Table 4. Computed parameters attached to duty points.

	Q_j [m³/s]	H_{Pj} [m]	η_j [−]	P_j [W]
pump P1	0.00099	14.20	0.372	372.1
pump P2	0.00099	14.18	0.372	372.2
pump P3	0.00100	14.14	0.371	372.6

For the computed pumped flow rates Q_j ($j = 1 \div 3$), one must verify if the pumps operate with or without cavitation when running at nominal speed.

The net positive suction head required by each pump, denoted $NPSH_{rj}$ with $j = 1 \div 3$, can be computed using the cavitation curve (3); the following values resulted: $NPSH_{r1} = 7.69$ m; $NPSH_{r2} = 7.70$ m; $NPSH_{r3} = 7.73$ m.

The net positive suction head available at the pump inlet is defined as [4]:

$$NPSH_{aj} = (p_i - p_v)/(\rho g) - (z_s - z_i) - \sum_k R_k Q_k^2 . \tag{9}$$

In (9), the index i designates a point on the free surface of the open tank R, where the elevation is $z_i = 0.77$ m and the atmospheric pressure is $p_i = 10.328$ mWC; the vapour pressure of water at 20°C is $p_v = 0.238$ mWC; all pumps have the same elevation $z_s = 0.23$ m at the centre of their suction section; the indexes k refer to pipes connecting the tank to the inlet of each pump, meaning that according to figure 1 and table 1, the head losses on the suction circuit are computed as following:

$$\sum_k R_k Q_k^2 = (R_4 + R_5)Q_5^2 + R_{3s}Q_3^2, \text{ for pump P3}$$
$$\sum_k R_k Q_k^2 = (R_4 + R_5)Q_5^2 + R_6 Q_6^2 + R_{2s}Q_2^2, | \text{ P2} \tag{10}$$
$$\sum_k R_k Q_k^2 = (R_4 + R_5)Q_5^2 + R_6 Q_6^2 + (R_7 + R_{1s})Q_1^2, | \text{ P1}$$

Inserting (10) into (9), the following values resulted: $NPSH_{a1} = 8.01$ m; $NPSH_{a2} = 8.02$ m; $NPSH_{a3} = 8.04$ m.

The non-cavitating operating condition [4], written as

$$NPSH_{aj} > NPSH_{rj} \qquad (11)$$

for $j = 1 \div 3$, is fulfilled for all pumps. Thus, for the designed configuration of the test rig, the operation of pumps at full capacity is safe, falling in the non-cavitating regime (for the considered pumping station, the nominal speed is the maximum speed reached by the pumps).

It's worth mentioning that decreasing the diameter of the main suction pipe (with index $j = 5$) is not an option, because the increase of the head losses on the suction circuit leads to cavitation in pumps: e.g. if the pipe 5 is of DN40 size, with an inner diameter $D_5 = 29.2$ mm, the solution of the system (7) gives $Q_1 = 0.000845$, $Q_2 = 0.000845$ and $Q_3 = 0.000846$ m³/s, as well as a minimal head $H_{21} = -9.02$ m near the inlet of pump P1; the NPSH available at the pump inlet (9) gives negative values.

4 Control methods based on PSP

In section 1 we highlighted two methods used to control the pumps operation based on the Pressure Set Point, namely:
• *classical PSP method* (commonly implemented by the water companies);
• *remote-control PSP method* (more expensive than the *classical* one, due to additional costs).

Theoretical aspects attached to the above control methods will be checked in this section, starting from the nonlinear system of equations (5), which was derived in section 3 for the experimental test rig, in the assumption that all pumps run at their nominal speed and all valves in the system are fully open.

4.1. Classical PSP method

The studied pumping station (PS) is equipped with a control panel with back-light display, function, navigation and operating keys. An adjustable PID-controller integrated in the software of the control panel [9] ensures that the system pressure remains constant, around the PSP level.

The standard operation of that PS relies on the *classical PSP method*: it is based on a pressure sensor on the discharge side of the PS, namely on the pipe 8 (figure 3), placed under a membrane pressure vessel (MPV). For a proper functioning of the PS, the air pressure in the membrane switch vessel must be adjusted to a correct value, which is 50 kPa lower than the switch-on pressure on the waterside [9].

The pumping station is presented in figure 3, where the network components were labelled as in figure 1.

Taking into account the nodal head values computed in nodes $22 \div 24$ (see table 3), and the elevation of 0.53 m at those nodes, the discharge pressure can be computed: $p_{22} \cong p_{23} \cong p_{24} = 1.24$ bar. Based on the pressure sensor accuracy (± 0.03 bar), we will assume further that the

PSP is compared to the pressure value of node 24, located at the PS exit.
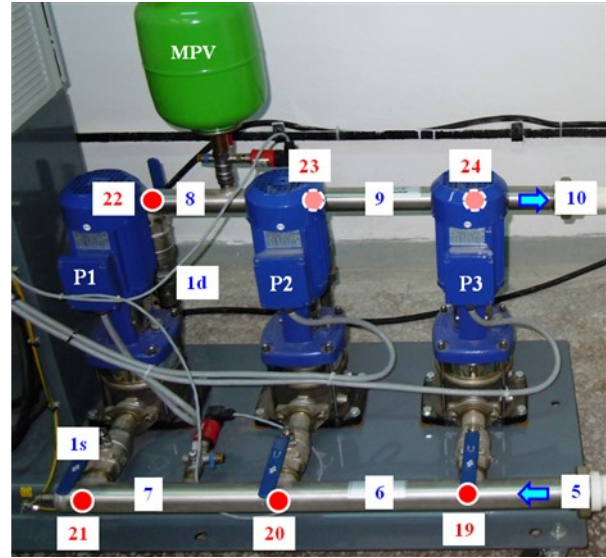
Fig. 3. Studied pumping station: pipes and nodes labelled as in figure 1, pumps P1 to P3, membrane pressure vessel MPV, pressure transducers on pipes 7 and 8 (pressure transducers, 0–6 bar, $\pm 0.5\%$ accuracy of full scale).

To verify how the PS responds to the *classical PSP method*, the system of equations (5) will be changed, based on the following assumptions: a head value at node 24 will be imposed, so H_{24} will be no more the 24th unknown of the system (5). It will be replaced by another unknown (let's say) the speed factor of pump P3. Thus, ω_3 will become the 24th unknown of the system (5), while $\omega_1 = \omega_2 = 1$ will be still considered. To solve the resulting system of equations, unknowns will be denoted as w_j with $j = 1 \div 31$, as follows:

$$
\begin{aligned}
w_1, \cdots, w_{17} &\equiv Q_1, \cdots, Q_{17} \\
w_{18}, \cdots, w_{23} &\equiv H_{18}, \cdots, H_{23} \\
w_{24} &\equiv \omega_3 \\
w_{25}, \cdots, w_{31} &\equiv H_{25}, \cdots, H_{31}
\end{aligned} \qquad (12)
$$

Thus, the functions f_3, f_9 and f_{10} of the system (7) will be changed. The new system to be solved is:

$$f_1 = w_{21} + 31.62\omega_1^2 - 17.625 \cdot 10^6 w_1^2 - w_{22} - R_1 w_1^2 = 0$$

$$f_2 = w_{20} + 31.62\omega_2^2 - 17.625 \cdot 10^6 w_2^2 - w_{23} - R_2 w_2^2 = 0$$

$$f_3 = w_{19} + 31.62 w_{24}^2 - 17.625 \cdot 10^6 w_3^2 - H_{24} - R_3 w_3^2 = 0$$

$$\ldots\ldots$$

$$f_9 = w_{23} - H_{24} - R_9 w_9^2 = 0 \qquad (13)$$

$$f_{10} = H_{24} - w_{25} - R_{10} w_{10}^2 = 0$$

$$\ldots\ldots$$

$$\text{if } (w_{31} - z_{31}) < p_{min}/(\rho g), \quad f_{31} = w_{17} = 0.$$

A value of H_{24} will be retrieved from previous data [10].

Dunca et al. [10] obtained experimental results on the same pumping station, controlled by the same *classical*

PSP method, but with the PS connected to a short closed-loop hydraulic circuit. We are interested now in selecting H_{24} values fitting the PS capabilities, if possible, values greater than the ones computed in table 3 − we would like to operate as close as possible to the pumps best efficiency point (53.7% [9]), not at some duty points of low efficiency as in table 4.

Among the 63 sets of data available from [10], we will focus only on 3 sets (see table 5), with $\omega_1 = \omega_2 = 1$ and $\omega_3 \neq 0$. For those sets, the PSP values (in bar) will be equivalent here to the pressure p_{24}, allowing us to compute the corresponding head: $H_{24} = (p_{24}/(\rho g) + z_{24})$. The total pumped flow rate established in [10] at the PS exit (equivalent to Q_{10} in the present paper) is added in table 5. The above flow rate was modified in [10] by throttling a discharge valve, with a certain value of the minor loss coefficient ζ. The control valve was of the same type and size as the TCV of pipe 14.

Table 5. Previous data corresponding to the studied PS [10].

p_{24} (PSP) [bar]	H_{24} [m]	ζ [−]	ω_3 [−]	Q_{10} [m³/s]
2.01	21.291	276/	0.8000	0.00171
2.34	24.699	179/	0.9883	0.00202
2.45	25.835	194/	0.9900	0.00188

To solve the system (13) attached to the *classical PSP method*, by imposing a high value of the head H_{24} (as in table 5), it is compulsory to decrease the total pumped flow rate with respect to $Q_{10} \cong 0.003$ m³/s from table 3. Thus, a minor loss coefficient $\zeta > 0$ at the TCV on pipe 14 will be set, which will increase the hydraulic resistance in the function f_{14} of (13), with respect to (7).

The numerical results, obtained after solving the system (13) for $H_{24} = 25.835$ m (PSP = p_{24} = 2.45 bar) and $\zeta = 513$ (bigger than the value from table 5), are presented in table 6.

Table 6. Solution of the system (13): Q_j for $j = 1\div17$, H_j for $j = 18\div23 \cup 25\div31$, and ω_3, for $H_{24} = 25.835$ m and $\zeta = 513$.

$w_j = Q_j$ for $j = 1\div17$ [m³/s]			Q_j [m³/h]	$w_j = H_j$ for $j = 18\div23$ and $j = 25\div31$ [m]	
w_1	Q_1	0.00058	2.096	w_{18}	H_{18}	0.680
w_2	Q_2	0.00058	2.097	w_{19}	H_{19}	0.232
w_3	Q_3	0.00058	2.094	w_{20}	H_{20}	0.225
w_4	Q_4	0.00175	6.287	w_{21}	H_{21}	0.223
w_5	Q_5	0.00175	6.287	w_{22}	H_{22}	25.844
w_6	Q_6	0.00116	4.193	w_{23}	H_{23}	25.842
w_7	Q_7	0.00058	2.096	w_{25}	H_{25}	22.104
w_8	Q_8	0.00058	2.096	w_{26}	H_{26}	21.994
w_9	Q_9	0.00116	4.193	w_{27}	H_{27}	21.840
w_{10}	Q_{10}	0.00175	6.287	w_{28}	H_{28}	21.713
w_{11}	Q_{11}	0.00148	5.315	w_{29}	H_{29}	21.883
w_{12}	Q_{12}	0.00121	4.343	w_{30}	H_{30}	21.804
w_{13}	Q_{13}	0.00094	3.371	w_{31}	H_{31}	21.626
w_{14}	Q_{14}	0.00094	3.371	w_{24}	ω_3	0.9995
w_{15}	Q_{15}	0.00027	0.972	$p_{29}/(\rho g)$ [m]		20.528
w_{16}	Q_{16}	0.00027	0.972	$p_{30}/(\rho g)$ [m]		20.749
w_{17}	Q_{17}	0.00027	0.972	$p_{31}/(\rho g)$ [m]		20.341

The system of equations (13) was solved for 4 pairs of the input values $\{H_{24}; \zeta\}$, starting with the same initial solution **w0** as for (7). Near the 3 head values from table 5, the head value of 18.695 m (which was the minimal value tested in [10]) was additionally added. For all cases, pumps run without cavitation. The computed results are synthesised in table 7, namely the speed factor ω_3, the total discharge flow rate Q_{10}, the head in node 28 (at the end of the main discharge pipe), pumps efficiency values η_j ($j = 1\div3$) and the total power consumed for pumping, P_T.

Obviously, by imposing such high values for H_{24}, the available pressure at each consumer is greater than the reference pressure, so according to (4), all three outflows equal the requested demand.

Table 7. Computed results based on the solution of system (13), where PSP = p_{24}, for different pairs of values $\{H_{24}; \zeta\}$.

p_{24} (PSP) [bar]	1.81	2.01	2.34	2.45
H_{24} [m]	18.695	21.291	24.699	25.835
ζ [−]	66.5	134.5	349.5	513
ω_3 [−]	0.9993	0.9993	0.9995	0.9995
Q_{10} [m³/s]	0.00253	0.00228	0.00189	0.00175
H_{28} [m]	9.940	14.228	19.844	21.713
$\eta_1 = \eta_2$ [−]	0.479	0.513	0.530	0.525
η_3 [−]	0.479	0.513	0.530	0.525
P_T [W]	989	934	862	837

4.2 Remote-control PSP method

In section 1, we mentioned that the *classical PSP method* ensures an excessive pressure across the WDN – that statement is sustained by the results from tables 6 and 7. The *remote-control PSP method* is supposed to reduce the pressure in the hydraulic system. To verify how the PS responds to the *remote-control PSP method*, the PSP will be compared to the pressure value in node 28 (the last node of the system). The nodal head is: $H_{28} = (p_{28}/(\rho g) + z_{28})$.

The procedure from subsection 4.1 will be repeated, pointing this time to H_{28}. Accordingly, the system (5) will be altered assuming that the head H_{28} is an input (imposed) value, while ω_3 becomes the 28th unknown in (5). To solve the new system of equations, the following notations will be used:

$$
\begin{aligned}
&w_1, \cdots, w_{17} \equiv Q_1, \cdots, Q_{17} \\
&w_{18}, \cdots, w_{27} \equiv H_{18}, \cdots, H_{27} \\
&w_{28} \equiv \omega_3 \\
&w_{29}, w_{30}, w_{31} \equiv H_{29}, H_{30}, H_{31}
\end{aligned}
\qquad (14)
$$

Based on (14), the functions f_3, f_{13} and f_{14} will change in (7), the new system of 31 equations $f_1 \div f_{31}$ being written:

$$f_1 = \ldots = 0, \quad f_2 = \ldots = 0$$

$$f_3 = w_{19} + 31.62 w_{28}^2 - 17.625 \cdot 10^6 w_3^2 - w_{24} - R_3 w_3^2 = 0$$

$$\ldots \quad f_{13} = w_{27} - H_{28} - R_{13} w_{13}^2 = 0 \qquad (15)$$

$$f_{14} = H_{28} - H_R - (R_{14} + R_v) w_{14}^2 = 0$$
$$..... \quad f_{31} = ... = 0.$$

Solving the system (15) for the input values from table 7, namely the head H_{28} and the coefficient ζ, will give the same results as the one obtained for the *classical PSP method*. That conclusion was predictable, since all 3 nonlinear systems of equations (7), (13) and (15) describe the same flowing phenomenon, based on the same physical laws. The only difference is the crossover of some input and output variables. Thus, for a given set of variables $\{\omega_3; \zeta; H_{24}; H_{28}\}$, leading to a proper operation of the test rig, the same solution (flow rates and nodal heads distributions) will be obtained by inserting $\{\omega_3; \zeta\}$ in (7), or $\{\zeta; H_{24}\}$ in (13), or $\{\zeta; H_{28}\}$ in (15).

Nevertheless, the system (15) attached to the *remote-control PSP method* can be solved, for input nodal heads H_{28} (let's say) at least half smaller than the values from table 7. One computation was performed for the PSP equal to the reference pressure: $p_{28} = p_{ref} = 2$ mWC = 0.19 bar. The computed results are synthesised in table 8. Here, pumps also run without cavitation.

Table 8. Computed results based on the solution of system (15), where PSP = p_{28}, for different pair of values $\{H_{28}; \zeta\}$.

p_{28} (PSP) [bar]	0.19 (p_{ref})	0.43	0.64	1.00
H_{28} [m]	2.530	4.970	7.114	10.857
ζ [−]	8.16	22.75	38.7	77.86
ω_3 [−]	0.9984	0.9984	0.9987	0.9990
Q_{10} [m³/s]	0.00291	0.00279	0.00268	0.00248
H_{24} [m]	14.214	15.682	16.980	19.247
$\eta_1 = \eta_2$ [−]	0.392	0.424	0.449	0.487
η_3 [−]	0.392	0.424	0.449	0.487
P_T [W]	1091	1055	1025	977

In table 8, for the last 3 input values of PSP = p_{28}, namely $p_{28} \in [0.43; 0.64; 1]$ bar, the available pressure at all consumers exceeds the p_{ref} level, so all three available outflows equal the requested demand: $Q_{aj} = Q_r = 0.972$ m³/h for $j = 29 \div 31$. For the critical PSP value $p_{28} = p_{ref} = 0.19$ bar, the pressure at the last consumer drops below p_{ref}, so the available outflows are: $Q_{a29} = Q_{a30} = Q_r$ and $Q_{a31} = 0.891$ m³/h.

4.3. Discussions

All numerical results obtained in this paper (in section 3, as well as in subsections 4.1 and 4.2) are verifying, from the mathematical point of view, each system of equations (7), (13) and (15), as pointed above.

The variation of the computed values of the nodal head H_{24} with respect to the total discharge flow rate Q_{10}, and the variation of the total power P_T consumed for pumping with respect to Q_{10} are plotted in figures 4 and 5, respectively (a total of 9 points are plotted, issued from tables 3, 7 and 8).

Within a pumping station where pumps are working in parallel coupling, the parallel operation point [4, 10] is defined by the pair of parameters, which consist of the

nodal head at the PS exit (in our case, H_{24} in node 24) and the total pumped flow rate (in our case, Q_{10}). As one can see in figure 4, the parallel operation points follow a decreasing trend, with increasing total discharge flow rate (it is the natural trend of the parallel coupling head – flow rate curve).
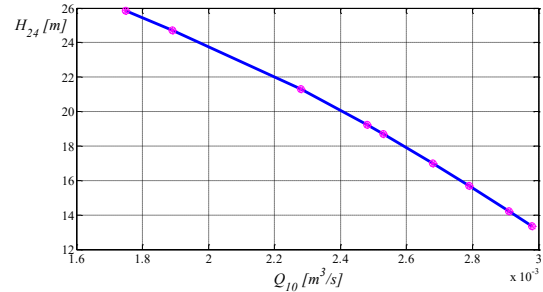
Fig. 4. Nodal head at the PS exit: $H_{24} = H_{24}(Q_{10})$.
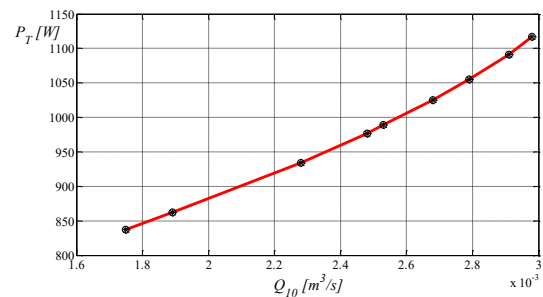
Fig. 5. Total power consumed for pumping: $P_T = P_T(Q_{10})$.

According to the curve plotted in figure 5, the parallel operation points follow an increasing trend of the power, with increasing pumped flow rate.

From the theoretical study conducted in this paper, the following concluding remarks emerge:

• the nonlinear systems of equations (7), (13) and (15) describe the physics of the same hydraulic process, thus they provide the same solution for a given set of variables $\{\omega_3; \zeta; H_{24}; H_{28}\}$, where different 2 out of 4 variables are inserted as input parameters in those systems, while the remaining 2 variables are unknowns;

• since all 3 nonlinear systems of equations (7), (13) and (15) are determined, the solver [16] converges for any starting guess, e.g. for a (non-physical) null initial solution;

• mathematically, one can test with various sets of variables $\{\omega_3; \zeta; H_{24}; H_{28}\}$, but the studied pumping station has some limitations (protections) for low pumping heads (where pumps run at low efficiency), as well as for low rotational speeds. Previous tests [10] were performed for $H_{24} \in [18.695; 25.835]$ m; for the network from figure 1, such values will ensure the final nodal heads $H_{28} \in [9.94; 21.713]$ m, which are greater than the critical value of 2.53 m from table 8; so, it might be difficult to set (to impose) experimentally too small H_{24} or H_{28} values, through one of the PSP control methods;

• for the tested nodal head values $H_{24} \in [15.682; 25.835]$ m, correlated with $H_{28} \in [4.97; 21.713]$ m (see tables 6, 7 and 8), the available outflow at all 3 consumers equals

the requested demand (due to the relation $p_j > p_{ref}$ for $j = 29 \div 31$);

• for two tested nodal head values, the pressure drops at all consumers (for $H_{24} = 13.346$ m, $H_{28} = 0.829$ m in table 3), or only at the last consumer (for $H_{24} = 14.214$ m, $H_{28} = 2.53$ m in table 8), so those pressure-deficient consumers receive a smaller outflow than the requested one;

• within the present study, all 3 pumps are working at nominal speed or near the nominal speed; the presented theoretical approach can be extended to the case where a single pump, or only 2 pumps are running.

5 Conclusions

In this paper, two methods used to control the pumps operation in pumping stations were termed as: *classical PSP method* and *remote-control PSP method*.

This paper focuses on the theoretical approach and numerical results linked to the design of an experimental test rig, intended to verify in the future if there is any advantage of the *remote-control PSP method*, with respect to the *classical PSP method*. Commonly, water companies implement the *classical method*, since the *remote-control method* implies additional costs.

The experimental facility, designed as presented here, already exists [8]. It consists of a pumping station with 3 parallel-coupled variable speed driven pumps (previously studied [10]), and a new piping network with 3 consumers (each with its throttling control valve, allowing to set different outflow rates). The present theoretical study was conducted assuming that all 3 pumps are working at nominal speed or near it, that valves are fully open at all consumers, and that the final discharge valve can be throttled from fully open to partially closed (through different minor loss coefficient values).

From the mathematical point of view, the nonlinear systems of equations describing the operation of the above test rig show that both PSP control methods are equivalent (so, one cannot claim that one is better than the other). Further experiments on the above test rig will highlight advantages and disadvantages of both control methods. Nevertheless, the present theoretical study offers enough data, useful to properly conduct the future experimental work.

References

1. J. Thornton, A. Lambert, IWA Water21, Dec., 24 (2006) https://www.waternz.org.nz/id=217

2. Á. Martínez-Codina, L. Cueto-Felgueroso, M. Castillo, L. Garrote, J. Water Res. Pl.-ASCE, **141**(9), (2015) doi:10.1061/(ASCE)WR.1943-5452. 0000519

3. R. Gomes, A. Sá Marques, J. Sousa, Urban Water J., **8**(2), 65 (2011) https://doi.org/10.1080/1573062X. 2010.542820

4. S.-C. Georgescu, A.-M. Georgescu, *Hydraulic networks analysis using GNU Octave*, in Romanian

(Printech Press, Bucharest, 2014) https://www. researchgate.net/publication/303805379

5. A.-M. Georgescu, S. Perju, S.-C. Georgescu, A. Anton, Procedia Engineering, **70**, 707 (2014) https://doi.org/10.1016/j.proeng.2014.02.077

6. S.-C. Georgescu, A.-M. Georgescu, R.A. Madularea, V.-F. Piraianu, A. Anton, G. Dunca, Procedia Engineering, **119**, 660 (2015) https://doi. org/10.1016/j.proeng.2015.08.919

7. S.-C. Georgescu, A.-M. Georgescu, R.A. Madularea, D.M. Bucur, G. Dunca, Environ. Eng. Manag. J., **16**(5), 1071 (2017) http://www.eemj. icpm.tuiasi.ro/issues/vol16/vol16no5.htm

8. Hydraulic Machinery Laboratory, WaterSIM-UPB, https://erris.gov.ro/WaterSiM---UPB (2018)

9. ***, *Hydro-Unit utility MCMF − Installation and operating instructions*, DP-Pumps, The Netherlands, http://www.dp-pumps.com/ (2012)

10. G. Dunca, V.-F. Piraianu, R. Roman, P.-O. Ciuc, S.-C. Georgescu, Energy Procedia, **112**, 100 (2017) https://doi.org/10.1016/j.egypro.2017.03.1070

11. G. Germanopoulos, *Civ. Eng. Syst.*, **2**(3), 171 (1985) https://doi.org/10.1080/02630258508970401

12. O. Giustolisi, D. Savic, Z. Kapelan, J. Hydraul. Eng., **134**(5), 626 (2008) https://doi.org/10.1061/ (ASCE)0733-9429(2008)134:5(626)

13. A.-M. Georgescu, S. Perju, R.A. Madularea, S.-C. Georgescu, Energy consumption due to pipe background leakage in a district water distribution system in Bucharest, *IEEE Conf. Publications, 2017 Int. Conf. on Energy and Environment CIEM* (2017) https://ieeexplore.ieee.org/document/8120785/

14. P.K. Swamee, A.K. Jain, J. Hydraul. Eng. Division, **102**(5), 657 (1976)

15. J.W. Eaton, D. Bateman, S. Hauberg, R. Wehbring, *GNU Octave. A high-level interactive language for numerical computations*, 4th ed. Octave 4.4.1 (2018) https://octave.org/octave.pdf

16. ***, *MATLAB Documentation/ Optimization toolbox/ Systems of nonlinear equations/ fsolve* (2018) https://www.mathworks.com/help/optim/ug/ fsolve.html